Tong-fu-li-fei decoction attenuates immunosuppression to protect the intestinal-mucosal barrier in sepsis by inhibiting the PD-1/PD-L1 signaling pathway

LI CHEN*, LAN LI*, SUZHAO ZOU, QIANHUA LIAO and BO LV

Department of Intensive Care Unit, First Affiliated Hospital of Guizhou University of Chinese Medicine, Guiyang, Guizhou 550001, P.R. China

Received August 29, 2020; Accepted March 1, 2021

DOI: 10.3892/mmr.2021.12480

Abstract. The aim of the present study was to investigate the therapeutic effects of Tong-fu-li-fei (TFL) decoction on sepsis-induced injury to the intestinal mucosal barrier and the underlying mechanism. Cecal ligation and puncture (CLP) was used to establish a sepsis model in rats. The post-surgery death of the rats was recorded to calculate the survival rate. A 4-kD fluorescein isothiocyanate (FITC)-dextran assay was used to evaluate the intestinal permeability of the rats. The pathological state of the intestine tissues was detected by hematoxylin and eosin staining and the ultrastructural changes in the endometrium were evaluated by transmission electron microscopy. Enzyme-linked immunosorbent assay was used to determine the concentrations of interleukin (IL)-6 and tumor necrosis factor (TNF)-α in the intestinal tissues and cells. The expression levels of SHP-2 and PI3K were detected by reverse transcription-quantitative PCR and western blotting. Sorting by flow cytometry was used to obtain pure dendritic cells (DC), $CD8^+$ T cells and natural killer cells. Western blotting was used to evaluate the expression levels of phosphorylated (p)-AKT and AKT. The results demonstrated that the significantly decreased survival rate caused by CLP surgery was elevated by glutamine (Gln) and TFL treatment. Intestinal permeability was increased by CLP, and greatly suppressed by Gln or TFL treatment. Histopathological changes in the intestinal tissues, such as thinner barrier and atrophied mucosa, and ultrastructure changes such as sharply decreased microvilli and mitochondria dropsy, were observed on sepsis animals; these effects were ameliorated by the introduction of Gln or TFL. The upregulation of SHP-2, PI3K and p-AKT induced by CLP was reversed by TFL. The release of IL-6 and TNF-α was elevated and the expression of SHP-2, PI3K and p-AKT was suppressed in the co-cultural system of DC cells and $CD8^+$ T cells by TFL. Overall, TFL decoction may attenuate immunosuppression to protect intestinal mucosal barrier in sepsis via inhibiting the programmed death1/programmed cell death ligand 1 signal pathway.

Introduction

Sepsis is a type of disease derived from systemic immune response to infection, which results in the death of 210,000 people annually in America as one of the main factors that contribute to the death of critically sick patients (1). The mortality of sepsis is ~30-70% (2). Currently, no effective therapeutic method is available to decrease the mortality of sepsis clinically. Therefore, it is of great significance to explore the detailed pathological mechanism of sepsis to provide novel therapeutic methods for the treatment of clinical sepsis.

A series of immune reactions can be induced by sepsis, which change as the time goes on (3). It is recently reported that pro-inflammatory reaction and anti-inflammatory reaction occur simultaneously under sepsis pathological state, with overactive immune response as the primary characteristic. According to the clinical data, most patients survived at the stage of overactive immune response, rather than at the stage of immunosuppression, which is manifested as a tardy response to antigen and incapable of eliminating secondary infection induced by primary infection (4). It is widely reported that apoptosis plays an important role in the immunosuppression response. Severe apoptosis was found on lymphocytes, parenchymatous cells and vascular endothelial cells isolated from sepsis animal models (5), which induce significant immunosuppression clinically and make patients more susceptible to the infection by pathogenic bacteria such as *pseudomonas aeruginosa* and *candida*. Apart from apoptosis, the dysfunction of monocytes also plays a significant role in immunosuppression. In the primary immune response post bacterial infection, monocytes defense the body from infection by phagocytizing microorganisms, detecting the

Correspondence to: Dr Bo Lv, Department of Intensive Care Unit, First Affiliated Hospital of Guizhou University of Chinese Medicine, 71 Baoshan North Road, Yunyan, Guiyang, Guizhou 550001, P.R. China
E-mail: yishenglvbo@163.com

*Contributed equally

Key words: Tong-fu-li-fei decoction, PD-1/PD-L1, sepsis, intestinal barrier, immunosuppression

metabolism of microorganisms, response to stimulators from microorganisms and producing numerous pro-inflammatory factors, such as interleukin (IL)-6 and tumor necrosis factor (TNF)-α (6). Under normal physiological state, circling monocytes are recruited back to the marrow to be differentiated to peripheral tissues, which support the survival of macrophages and dendritic cells (DC). The immunosuppression induced by sepsis can be regulated by both the primary immune and secondary immune system. In addition, the acquired immunity system can be built by antigen presenting cells (APC) through stimulating the response of specific T cells (7,8). However, under the immunosuppression state induced by sepsis, dysfunction of monocytes against bacterial infections was observed. Furthermore the antigen-presenting ability of APC will be inhibited by the downregulation of human leukocyte antigen DR (HLA-DR) (9,10). Therefore, regulating the response of monocytes to immunosuppression induced by sepsis is very important to explore novel therapeutic routine for the treatment of sepsis.

Programmed death 1 (PD-1) was firstly found in the programmed dead cell lines using subtractive hybridization technology by Ishida *et al* (11), which belongs to type I transmembrane glycoproteins in immunoglobulin superfamily with a molecular weight of 55 kDa. PD-1 is highly expressed on T cells, B cells, myeloid cells and thymocytes, which regulates the immune system negatively (12). It is widely reported that PD-1/programmed cell death ligand 1 (PD-L1) signaling pathway is involved in immunologic tolerance in peripheral tissues and plays an important role in the development of chronic virus infection, inflammation, tumor immunity and autoimmune disease by mediating its downstream signal pathways, such as PI3K/AKT and SHP-2 signal pathway (13,14). Some progress has already been made on weakening, restricting or terminating the function of effective T cells by interacting with the PD-1/PD-L1 signal pathway (15). Tong-fu-li-fei (TFL) decoction is a traditional Chinese recipe that has already been proved to elicit therapeutic effects on sepsis (16). However, the underlying mechanism remains unknown, particularly its effects on immunosuppression induced by sepsis. In the present study, the effects of Tong-fu-li-fei decoction on PD-1/PD-L1 axis, as well as the downstream signaling pathway, will be investigated to explore the potential mechanism underlying the therapeutic property of Tong-fu-li-fei decoction on sepsis. Supportive pre-clinical data will be provided by the present study for the clinical treatment of sepsis with Tong-fu-li-fei decoction.

Materials and methods

Preparation of TFL decoction. TFL prescription was obtained from a national medical master Professor Liu Shangyi. The TFL prescription including 8 herbs, as shown in Table I, which were purchased from Sinopharm Group Tongjitang Pharmaceutical Co. Ltd, provided by a pharmacy from the First Affiliated Hospital of Guiyang College of Traditional Chinese Medicine. The extraction process was as follows: *Rheum officinale*, mirabilite, *Magnolia officinalis*, Forsythia, Scutellaria, almond, Bletilla striata and notoginseng (quality ratio of herb=2:1:1:1:1:1:1:1) were immersed in distilled water (1 g: 20 ml) and boiled gently for 1 h twice. The resulting extracts were filtered, combined, condensed into 1 g/ml (the content of crude drug in the decoction), and stored at 4˚C before use.

Animals. One-hundred male Sprague-Dawley rats weighing 200-220 g were procured from Vital River Laboratory Animal Co. Ltd. and group housed in polypropylene cages. The animal room environment was controlled (target conditions: Temperature, 20 to 26˚C; relative humidity, 30 to 70%' 12-h artificial light and 12-h dark). Temperature and relative humidity was monitored daily. The light cycle may have been interrupted for facility or study-related procedures. The rats were fed by standard dry rat diet and pure water. To minimize the animal suffering, we replaced the wood filings in the cage every day during the experimental procedures.

Establishment of the sepsis model by cecal ligation and puncture (CLP) in rats and treatment. The rats were anesthetized by an abdominal injection of 3% pentobarbital sodium (30 mg/kg). Surgery was performed under sterile conditions. A midline abdominal incision was performed and the cecum was exposed and the distal 1/3 was ligated with a 3-0 silk. At the end of the appendix, two holes were punctured with an 18-gauge needle. The cecum was then replaced in its original position within the abdomen, which was closed in two layers (in sham group, cecum was replaced). Surgery lasted for 20 min. Warm Ringer's lactate (50 ml/kg) with buprenorphine (0.01 mg/kg) was administered subcutaneously via abdominal wall. Immediately after the surgical operation, animals received an oral gavage of normal saline in the sham group (n=6) and model group (n=6), 750 mg/kg glutamine (n=6), 7 ml/kg (n=6), 14 ml/kg (n=6), and 28 ml/kg Tong-fu-li-fei decoction (n=6), respectively.

Symptoms and signs of rats. The symptoms of the rats were observed postoperatively. To determine the effect of TFL on mortality from CLP-induced sepsis, survival after CLP was assessed four times a day for at least 7 days and the cumulative survival curve was plotted using the Kaplan-Meier method (17).

FD4 detection. A 4-kD fluorescein isothiocyanate (FITC)-dextran (FD4; Sigma-Aldrich; Merck KGaA) solution was used for intestinal permeability measurement (18). Briefly, 20.8 mM solution of FD4 was prepared with sterile distilled water using colored Eppendorf tubes to keep away from light. The FD4 solution was gently administered as oral gavage to rats in each group at 10 ml/g bodyweight. Rats were held in an upright position for about 10 sec to avoid regurgitation. Blood (0.5-1 ml) was collected into an EDTA-loaded vacuum tube, and plasma samples were separated immediately by spinning down in a refrigerated centrifuge (1,000 x g for 30 min at 48˚C). Then, plasma samples were added to a black 96-well microplate. The FITC concentration was measured using a Microplate spectrophotometer with an excitation wavelength of 485 nm and an emission wavelength of 535 nm. In addition, a serial dilution of FITC was prepared and used for a standard curve. The plasma obtained from control group was used as a negative control.

Hematoxylin and eosin (H&E) staining. After FD4 detection, 200 mg/kg phenobarbital sodium was administered

Table I. Herbs included in the Tong-fu-li-fei (TFL) prescription.

Latin name	Chinese name	Weight of crude drug, g	Quality ratio
Rheum officinale Baill	Dahuang	20	2
Mirabilite	Mangxiao	10	1
Magnolia officinalis Rehd. et Wils	Houpo	10	1
Forsythia suspensa (Thunb.) Vahl	Lianqiao	10	1
Scutellaria baicalensis Georgi	Huangqin	10	1
Prunus armeniaca L. var. ansu Maxim	Kuxingren	10	1
Bletilla striata (Thunb.) Reichb. F	Baiji	10	1
Panax notoginseng (Burk.) F. H. Chen	Sanqi	10	1

intraperitoneally for euthanasia in rats. The intestinal mucosa tissue of each animal was collected and washed over by sterile water for a couple of hours. The tissue was dehydrated by 70, 80 and 90% ethanol solution successively and mixed with equal quantity of ethanol and xylene. After 15-min incubation at room temperature, the tissue was mixed with equal quantity of xylene for 15 min at room temperature. The step was repeated until the tissue looked transparent. Subsequently, the tissue was embedded in paraffin, sectioned (4 μm), and stained with H&E at room temperature for 30 min. Images were captured using an inverted light microscope (magnification, x50 and x100; Olympus Corporation). The H&E staining score was evaluated according to the colon mucosa damage index system described previously (19). Briefly, 0 point represented no injury to the intestinal mucosa; 1 point indicated that the surface of the intestinal mucosa was smooth, with no erosion or ulceration, but with mild hyperemia and edema; 2 points indicated that the intestinal mucosa had congestion and edema, and the mucosa was coarse and granular, with erosion or intestinal adhesion; 3 points indicated necrosis and ulcers appeared on the surface of intestinal mucosa, which also exhibited high congestion and edema (maximum longitudinal diameter of the ulcer, <1.0 cm), the intestinal wall surface also had necrosis and inflammation or hyperplasia of the intestinal wall was detected; 4 points indicated that the maximum longitudinal diameter of the ulcer was >1.0 cm with total intestinal wall necrosis more severe than that observed at 3 points.

Transmission electron microscope (TEM). Intestinal mucosa tissue was collected after the animals were euthanized and was fixed with 2.5% glutaraldehyde for >2 h and washed over by 0.1 M phosphoric acid solution for 3 times. Then, the tissues were fixed with 1% osmic acid for 2-3 h and washed over by 0.1 M phosphoric acid solution for 3 times. Ethyl alcohol (50, 70, 90 and 90%) and 90% acetone (v:v=1:1), 90% acetone were used to wash out the tissues for 15-20 min, successively. Subsequently, the tissues were incubated thrice with 100% acetone at room temperature for 15-20 min every time. Acetone (100%) and the embedding solution were used to incubate with the tissues for 3-4 h. Finally, the tissues were incubated with embedding solution in 37˚C oven overnight, 45˚C oven for 12 h and 60˚C oven for 48 h, successively. The solid tissues were cut into coronal sections (30 μm) and the slides were stained with 3% uranyl acetate and 3% lead citrate for 15 min at room temperature. Ultrastructural changes of endometrium were observed and photographed under transmission electron microscopy (JEM-1230; magnification, x20,000).

Transfection. The pc-DNA3.1-PD-1 and pc-DNA3.1-PD-L1 plasmids were designed and constructed by Genscript Technology. DC and $CD8^+$ T cells were transfected with pc-DNA3.1-PD-L1 (1.5 μg/well) combined with Lipofectamine® 3000 (Thermo Fisher Scientific, Inc.) at 37˚ for 48 h to establish the PD-L1 overexpressed DC and $CD8^+$ T cells. These transfected cells were utilized in the subsequent experiments 2 days later. The pc-DNA3.1-NC was used as a negative control.

Enzyme-linked immunosorbent assay (ELISA). According to the instruction of the manufacturer, the concentration of IL-6 (cat. no. RK00008; ABclonal Biotech Co., Ltd.) and TNF-α (cat. nos. RK00027; ABclonal Biotech Co., Ltd.) in the intestine mucosa tissue of each rat or the supernatant of cells was determined by ELISA. Basically, the operation includes: Sample adding, enzyme adding, incubation, working solution preparing, washing, dyeing, terminating, and detecting. Linear regression equation was described based on the concentration of standards and optical density (OD) value. The concentrations of the samples were calculated according to the equation, detected OD value and dilution factor.

Flow cytometry. After cells were counted, $2x10^6$ cells per sample were stained with Aqua Live/Dead viability dye (Thermo Fisher Scientific, Inc.), according to the manufacturer's instructions. Cells were then incubated in blocking solution containing 5% normal mouse serum, 5% normal rat serum, and 1% FcBlock (eBioscience; Thermo Fisher Scientific, Inc.) in PBS at 4˚C for 1 h, and then stained with a standard panel of immunophenotyping antibodies (CD11c, 1:800, cat. no. ab254183; CD80, 1:800, cat. no. ab134120; CD3, 1:1,000, cat. no. ab16669; CD8, 1:500, cat. no. ab217344 and DX5, 1:200, cat. no. ab181548; Abcam) for 30 min at room temperature. After staining, cells were washed and fixed with 0.4% paraformaldehyde in PBS at 4˚C for 24 h. Data was acquired with a BD LSRII flow cytometer using BD FACSDiva software (v 8.0.3; BD Biosciences). Compensation was performed on the BD LSRII flow cytometer at the beginning of each experiment. Data were analyzed using Flowjo v10 (FlowJo, LLC). Cell sorting for cytospins was

performed on a BD Aria II. The collected cells were stained with a Jenner-Giemsa Stain kit (ENG Scientific Inc.) at room temperature for 15-30 min and examined by light microscopy (magnification, x40).

Reverse transcription-quantitative PCR (RT-qPCR). Total RNA was collected from the intestine mucosa tissue from each rat or cells using an RNA Extraction kit (Takara Bio, Inc.) according to the manufacturer's instructions. The extracted RNA was quantified with a NanoDrop spectrophotometer (NanoDrop Technologies; Thermo Fisher Scientific, Inc.). A specific RT primer was used to reverse transcribe the complementary DNA at 50˚C for 45 min. SYBR Premix Ex Taq™ (Takara Bio, Inc.) with an Applied Bio-Rad CFX96 Sequence Detection system (Applied Biosystems; Thermo Fisher Scientific, Inc.) was used for the PCR procedure. PCR was conducted according to the following conditions: 95˚C for 5 min, followed by 40 cycles at 95˚C for 10 sec, 60˚C for 15 sec and 72˚C for 30 sec, and a final extension step at 72˚C for 5 min. The expression levels of SHP-2, PD-1, PD-L1 and PI3K was determined by the threshold cycle (Ct), and relative expression levels were calculated by the $2^{-\Delta\Delta Cq}$ method (20). The expression level of GAPDH in the tissue was considered for the normalization of mRNA expression. Three independent assays were performed. The information of the primers is shown in Table II.

Western blotting. Total proteins were isolated from tissues or cells using the Nuclear and Cytoplasmic Protein Extraction kit (Beyotime Institute of Biotechnology), and were quantified using the BCA kit (Beyotime Institute of Biotechnology). Approximately 40 μg of protein was separated on 12% SDS-polyacrylamide gel (SDS-PAGE) and the gel was transferred to polyvinylidene difluoride (PVDF) membrane (EMD Millipore). The membrane was blocked with 5% nonfat dry milk in TBST (Tris-buffered saline/0.1% Tween-20; pH 7.4) for 1 h at room temperature. The membrane was then incubated at 4˚C overnight with primary rabbit anti-human antibodies to PD-1 (1:1,000; cat. no. ab243644), PD-L1 (1:1,000; cat. no. ab205921), SHP-2 (1:1,000; cat. no. ab32083), PI3K (1:1,000; cat. no. ab32089), phosphorylated (p)-AKT (1:1,000; cat. no. ab8805), AKT (1:1,000; cat. no. ab38449) and GAPDH (1:1,000; cat. no. ab9485) (all from Abcam). A horseradish peroxidase-conjugated antibody against rabbit IgG (1:5,000; cat. no. ab7090; Abcam) was used as a secondary antibody. Blots were incubated with the ECL reagents (Beyotime Institute of Biotechnology) and exposed to Tanon 5200-multi to detect protein expression. ImageJ software 1.8.0. (National Institutes of Health) was used to semi-quantify the bands. Three independent assays were performed.

Statistical analysis. Data are expressed as mean ± SD, with the exception of HE score data, which are shown as median and range. Statistically significant differences for continuous variables were determined using a one-way analysis of variance (ANOVA) with Tukey's test for the normally distribution data. All analyses were performed using GraphPad Prism 5 software (GraphPad Software, Inc.). P<0.05 was considered to indicate a statistically significant difference.

Table II. Sequences of primers for SHP-2, PI3K and GAPDH.

Primer ID	Sequences (5'-3')
SHP-2 F	AGACCACCAGCCAAGACAAG
SHP-2 R	CTCCAGGTCCATCACCAAGT
PI3K F	ACACCACGGTTTGGACTATGG
PI3K R	GGCTACAGTAGTGGGCTTGG
GAPDH F	CAATGACCCCTTCATTGACC
GAPDH R	GAGAAGCTTCCCGTTCTCAG

F, forward; R, reverse.

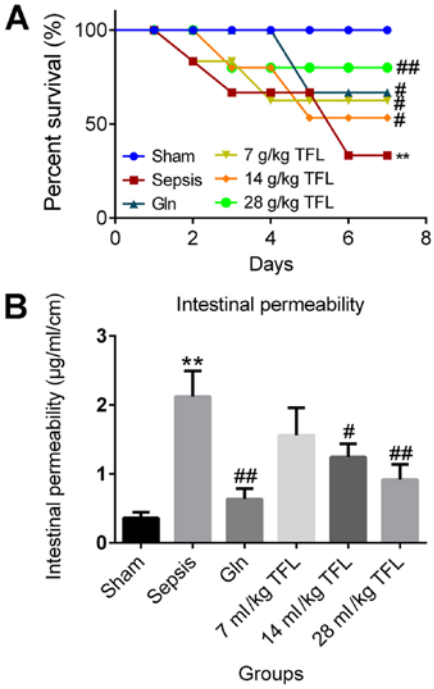

Figure 1. General symptom and survival rate of rats induced with cecal ligation and puncture are alleviated by TFL. (A) The survival rate of each group. (B) The intestinal permeability (μg/ml/cm) of each rat was evaluated by a 4-kD fluorescein isothiocyanate-dextran assay. **P<0.01 vs. sham; $^{\#}$P<0.05 vs. sepsis; $^{\#\#}$P<0.01 vs. sepsis. TFL, Tong-fu-li-fei; Gln, glutamine.

Results

General symptom and survival rate of CLP-induced rats are alleviated by TFL. No abnormal symptom was observed in animals in the sham group. Apparent pathological symptoms described by Wichterman *et al* (21) were found in CLP-induced rats. Such clinical observations include listless spirit, rolled up body, decreased movements and decreased water intake, which were recorded for animals in the sepsis group at the early stage post-surgery. As the time went on, the CLP rats showed low skin temperature, weakened muscle strength, excreted watery stool, yellow color, fishy smell, and developed shortness of breath, no resistance to passive supine and the feces were slimy and abundant, which were reversed significantly by the treatment of glutamine (Gln) and TFL. The data on the survival rate for each group was illustrated in Fig. 1A. The overall survival rate of animals in the sham group was maintained

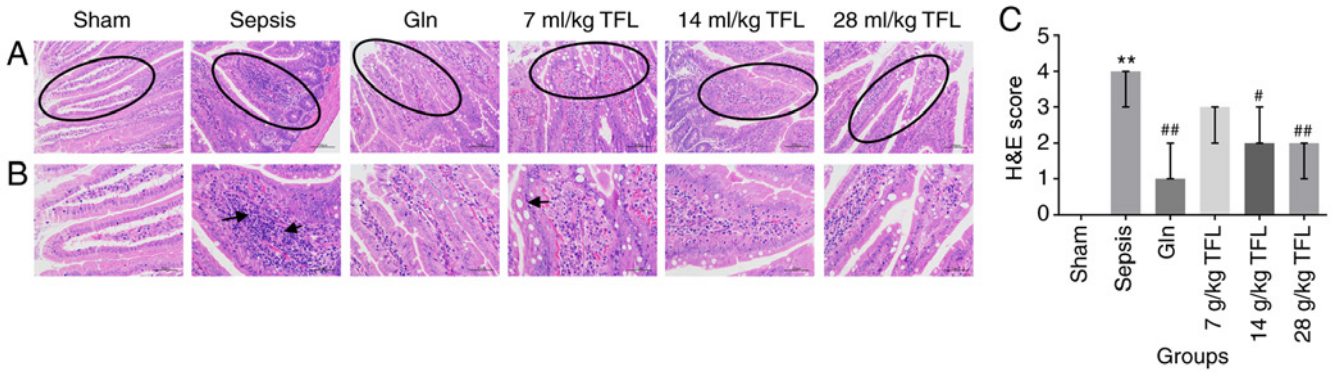

Figure 2. Histopathological state of intestinal tissues of each rat detected by H&E staining. Images were captured under a light microscope at magnifications, x200 (A) and x40 (B) The arrow represents the villous rupture. (C) Quantified pathological score of each group. **P<0.01 vs. sham; $^{\#}$P<0.05, $^{\#\#}$P<0.01 vs. sepsis. TFL, Tong-fu-li-fei; Gln, glutamine; H&E, hematoxylin and eosin.

as 100% in the 7 days post-surgery. However, significant decrease in the survival rate was observed in CLP-induced rats (**P<0.01 vs. sham), which was greatly ameliorated by the introduction of Gln and TFL, especially for high and moderate dosages of TFL ($^{\#}$P<0.05 vs. sepsis; $^{\#\#}$P<0.01 vs. sepsis). The intestinal permeability of each rat was further investigated to demonstration the potential toxicity. As shown in Fig. 1B, the permeability of intestine was significantly promoted in CLP-induced rats compared with the sham group (**P<0.01 vs. sham), which was greatly suppressed by the introduction of Gln and TFL (14 and 28 ml/kg) ($^{\#}$P<0.05 vs. sepsis; $^{\#\#}$P<0.01 vs. sepsis), respectively.

Effect of TFL on histopathology of intestinal tissues in CLP-induced rats. H&E staining was used to evaluate the pathological state of intestine tissue of each rat (Fig. 2). The rats in the sham group exhibited normally structured intestines under light microscope observation, without tissue edema, and presented with normal villus structure and clear edge of microvilli. Regarding the animals from sepsis group, the intestinal wall was noted to be thinner, the mucosa was atrophied, and local shedding and villous rupture (black arrows) were observed. The rats in the Gln, 14 and 21 ml/kg TFL group exhibited partial intestinal mucosal necrosis and shedding, but the intestinal mucosal lesions were relatively mild. These data claimed potential therapeutic effects of TFL on the injured intestinal tissues induced by CLP. In order to check the ultrastructural change in intestinal mucosa, TEM was performed on the intestinal mucosa tissues. In the sepsis group, the ultrastructure of intestinal epithelial cells showed decreased and deformed microvilli, and incomplete desmosomes (Fig. 3). The edema of the villi cells was more pronounced with the mitochondrial dropsy (black arrows) and vacuolar change, gaps of enterocytes were sharply widened, junctional complex among enterocytes were shortened and widened. In contrast, the ultrastructure from Gln, 14 and 21 ml/kg TFL-treated rats showed that the microvilli were dense and regular with a jagged and interlocking pattern among enterocytes and the mitochondria were clear.

TFL suppresses the inflammation and PD-1/PD-L1 signal pathway induced by CLP. To investigate the potential mechanism underlying the effects of TFL on the injured

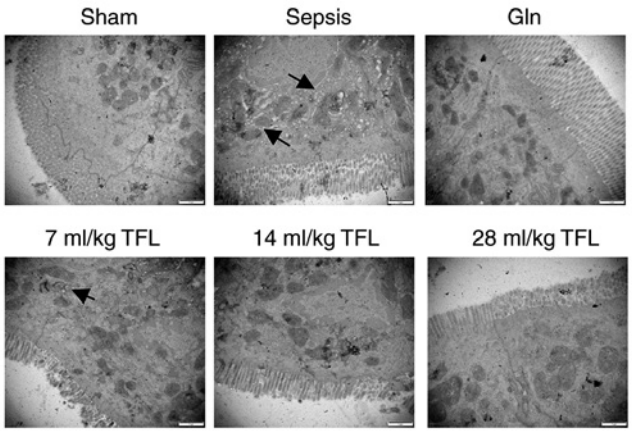

Figure 3. Ultrastructural changes in the endometrium were evaluated by transmission electron microscope (Scale bar, 500 nm). The arrows represent the mitochondrial dropsy. TFL, Tong-fu-li-fei; Gln, glutamine.

intestine induced by CLP, the concentration of IL-6 and TNF-α, as well as the expression level of key proteins involved in PD-1/PD-L1 signal pathway was determined in the intestine tissues. As shown in Fig. 4A, compared with the sham group, the concentration of IL-6 and TNF-α was elevated significantly in CLP-treated rats (**P<0.01 vs. sham), which was greatly suppressed by the treatment of Gln, 14 and 28 ml/kg TFL ($^{\#}$P<0.05 vs. sepsis; $^{\#\#}$P<0.01 vs. sepsis), respectively. SHP-2, PI3K and p-AKT were found to be significantly upregulated in CLP-induced rats (**P<0.01 vs. sham; Fig. 4B-C), which was downregulated by the introduction of Gln, 14 and 28 ml/kg TFL ($^{\#}$P<0.05 vs. sepsis, $^{\#\#}$P<0.01 vs. sepsis), respectively. In addition, it was found that the elevated expression level of PD-1 and PD-L1 in the intestine induced by CLP was significantly suppressed by the treatment of TFL in a dose-dependent manner ($^{\#}$P<0.05 vs. sepsis; $^{\#\#}$P<0.01 vs. sepsis; Fig. 4B-C).

TFL inhibits the release of inflammatory factors by blocking the PD-1/PD-L1 signal pathway. To further verify the inhibitory effects of TFL on inflammation through regulating the PD-1/PD-L1 signal pathway, DC cells, $CD8^+$ T cells and NK cells were isolated from the peripheral blood of rats, the phenotypes of which are shown in Fig. 5A.

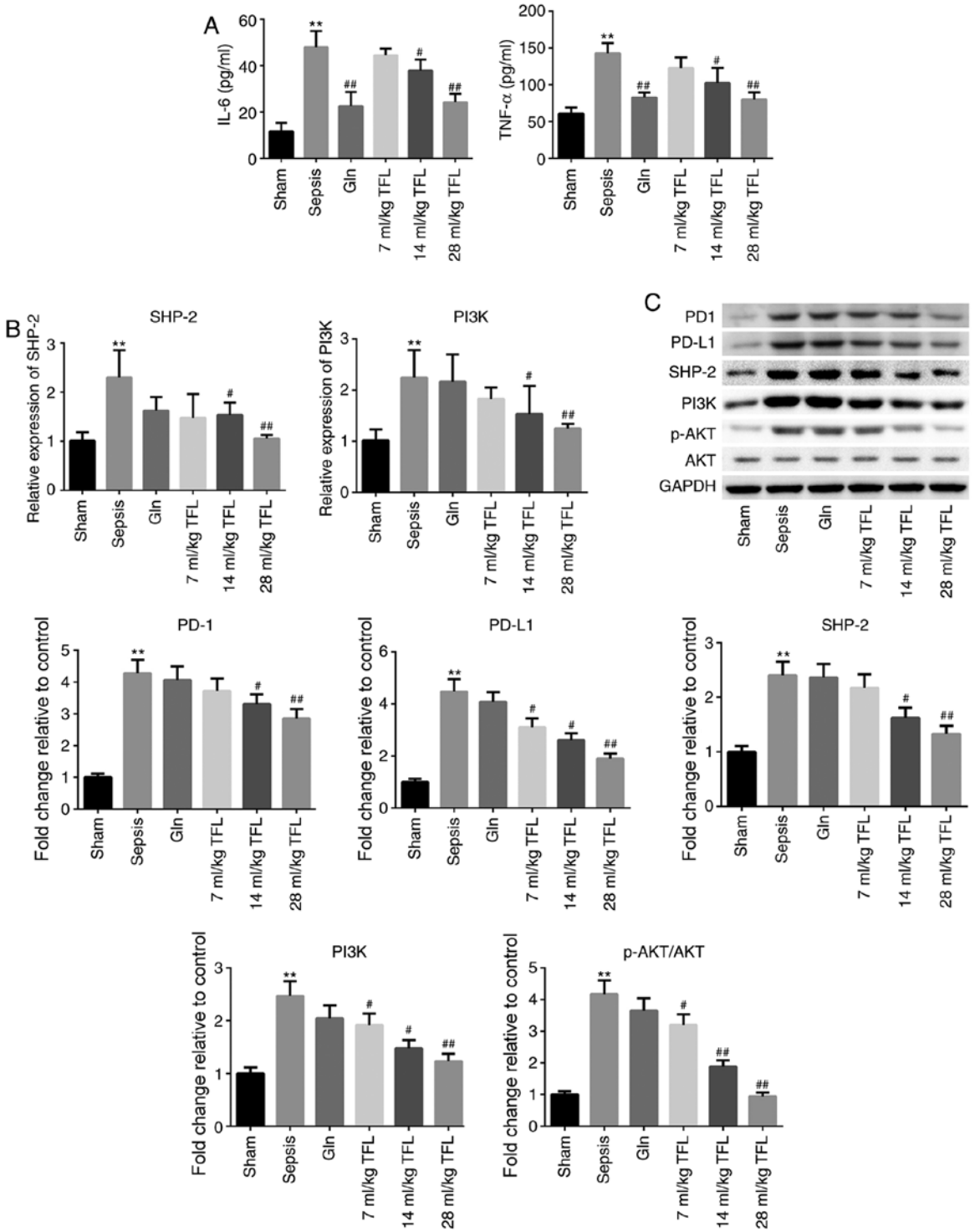

Figure 4. TFL suppresses the inflammation and PD-1/PD-L1 signal pathway induced by cecal ligation and puncture. (A) The concentration of IL-6 and TNF-α was determined by enzyme-linked immunosorbent assay. (B) The expression of SHP-2 and PI3K was evaluated by reverse transcription-quantitative PCR. (C) The expression level of PD-1, PD-L1, SHP-2, PI3K, p-AKT and AKT in the intestine was detected by western blotting. **P<0.01 vs. sham; $^{\#}$P<0.05 vs. sepsis; $^{\#\#}$P<0.01 vs. sepsis. IL-6, interleukin-6; TNF-α, tumor necrosis factor-α; PD-1, programmed death 1; PD-L1, programmed cell death ligand 1; p-, phosphorylated-; TFL, Tong-fu-li-fei; Gln, glutamine.

$CD11c^+CD80^-$ cells were isolated as DC cells, $CD3^+$ $CD8^+$ as $CD8^+$ T cells and $CD3^-DX5^+$ cells as NK cells by sorting flow cytometry. As shown in Fig. 5B, compared with DC cells, higher PD-1 expression level and lower PD-L1 expression level were observed both on $CD8^+$ T cells and NK cells, respectively. 0.01, 0.02, and 0.04 ml/ml TFL were incubated with the co-cultural system containing both DC cells and $CD8^+$ T cells. As shown in Fig. 6A, the production of IL-6 and TNF-α was significantly elevated by the introduction of 0.02 and 0.04 ml/ml TFL in a dose-dependent manner (*P<0.05 vs. control; **P<0.01 vs. control). Fig. 6B showed the expression level of key proteins in the downstream of PD-1/PD-L1 signal pathway. It was found that SHP-2, PI3K and p-AKT were significantly downregulated by the treatment of 0.02

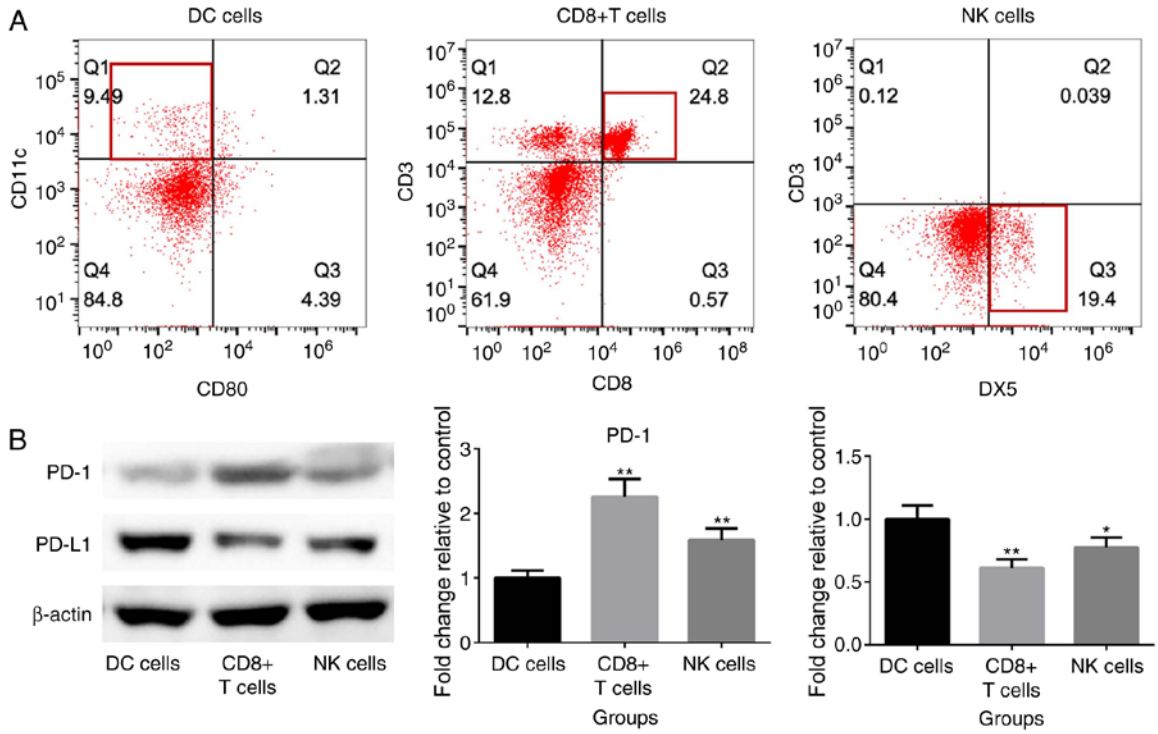

Figure 5. Expression level of PD-1 and PD-L1 in isolated DC cells, CD8+ T cells and NK cells. (A) The DC cells, CD8+ T cells and NK cells were sorted by sorting flow cytometry. (B) The expression level of PD-1 and PD-L1 in isolated DC cells, CD8+ T cells and NK cells was detected by western blotting. *P<0.05 vs. DC cells; **P<0.01 vs. DC cells. DC, dendritic cells; NK cells, natural killer cells; PD-1, programmed death 1; PD-L1, programmed cell death ligand 1.

and 0.04 ml/ml TFL in a dose-dependent manner (*P<0.05 vs. control; **P<0.01 vs. control).

To further verify the mechanism, the PD-L1 overexpressed DC cells and the PD-1 overexpressed CD8+ T cells were established, with DC cells transfected with pc-DNA3.1-NC and CD8+ T cells transfected with pc-DNA3.1-NC as negative control, respectively. As shown in Fig. 6C, compared with pc-DNA3.1-NC transfected DC cells, the expression level of PD-L1 was significantly elevated in pc-DNA3.1-PD-L1 transfected DC cells (**P<0.01 vs. pc-DNA3.1-NC). In addition, compared with pc-DNA3.1-NC transfected CD8+ T cells, the expression level of PD-1 was notably increased in pc-DNA3.1-PD-1 transfected CD8+ T cells (**P<0.01 vs. pc-DNA3.1-NC). Subsequently, four groups were formed: DC cells incubated with CD8+ T cells in the absence of 0.02 ml/ml TFL; DC cells incubated with CD8+ T cells in the presence of 0.02 ml/ml TFL; PD-L1-overexpressed DC cells incubated with CD8+ T cells in the presence of 0.02 ml/ml TFL; and DC cells incubated with PD-1-overexpressed CD8+ T cells. As shown in Fig. 6D, it was found that the suppressed expression of SHP-2, PI3K and p-AKT (induced by the introduction of TFL) was dramatically elevated by upregulating PD-L1 in the DC cells or upregulating PD-1 in the CD8+ T cells (**P<0.01 vs. control; ##P<0.01 vs. TFL). These data indicate that the regulatory effect of TFL on SHP-2 and PI3K/AKT signal pathway was associated with the inactivation of the PD-1/PD-L1 signal pathway.

Discussion

Sepsis is manifested as life-threating organic dysfunction induced by the imbalance of immune reaction following infection (22). It is currently suggested that inflammatory reaction and immunosuppression are involved in the whole pathological process of sepsis (23,24). Immunosuppression is the main factor that contributes to the secondary infection and multiple organ dysfunction syndrome diagnosed in patients with sepsis (25). Thus, ameliorating the immunosuppression state may be beneficial to the treatment of clinical sepsis. Intestinal injury is one of the main pathological characteristics of sepsis, which significantly influences the health of patients with sepsis (26). In the present study, a sepsis model was established by CLP in rats to simulate the pathological state of sepsis-induced intestinal barrier injury. The CLP-induced rat model was confirmed by significantly low survival rate, elevated intestinal permeability, histopathological changes in intestinal tissues, such as thinner barrier, atrophied mucosa, local shedding and villous rupture, and ultrastructure changes, such as sharply decreased microvilli, mitochondrial dropsy, vacuolar changes, widened gaps of enterocytes, and shortened junctional complex among enterocytes. In addition, severe inflammation was observed in the intestinal tissues of CLP-induced rats. Gln, which showed significant effects in preventing intestinal injury caused by external stimulations (27,28), was used as a positive control in the present study. A high, moderate, and low dosage of TFL was administered to the CLP-induced rats orally. It was found that the total survival rate was promoted by both Gln and TFL, especially at the high dosage. The enlarged permeability induced by CLP was suppressed by both Gln and TFL, indicating a potential repair function of TFL on injured intestine tissues caused by CLP. The alleviating effects were verified by ameliorated pathological state and ultrastructure changes in endothelial

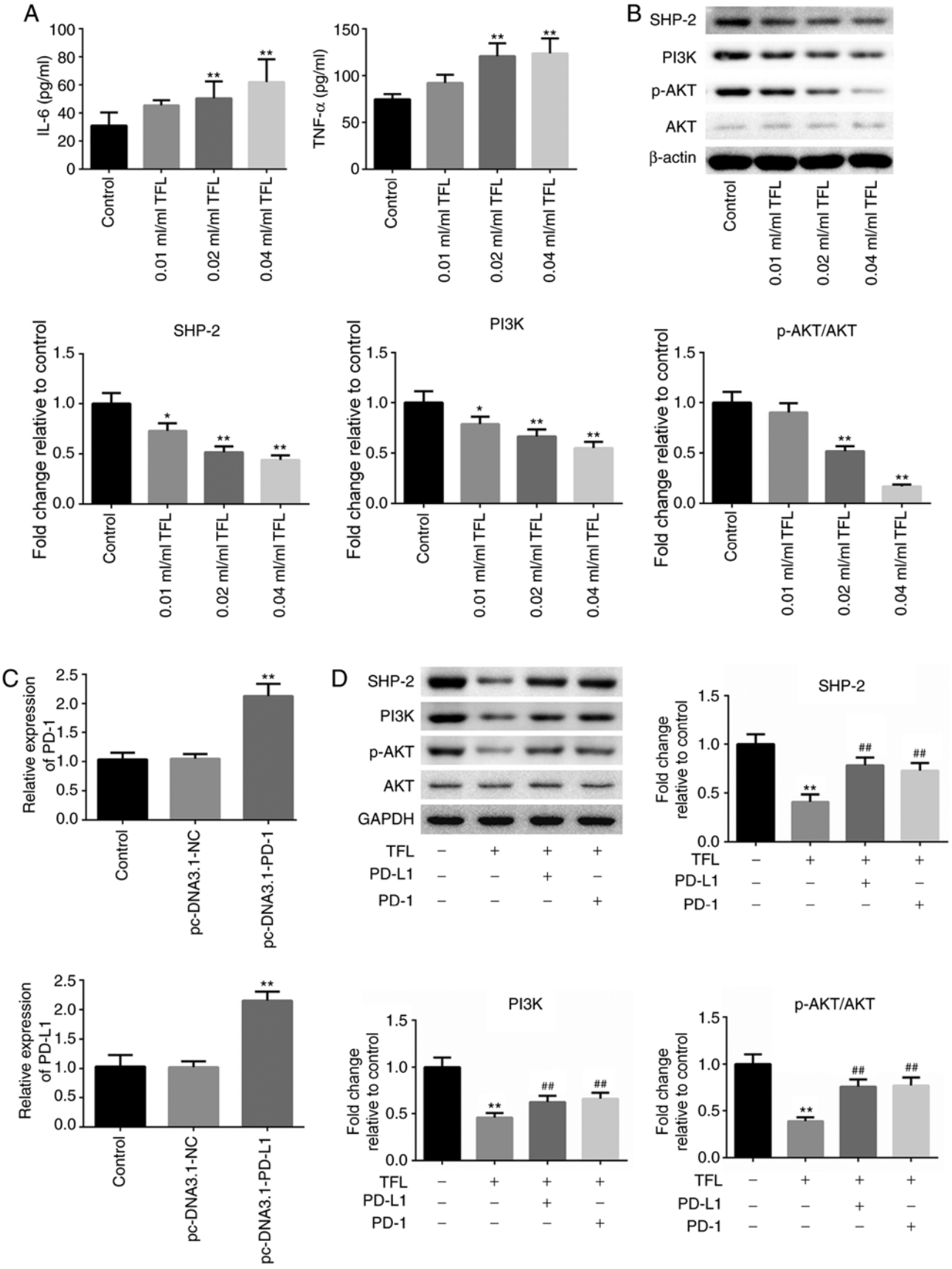

Figure 6. TFL inhibits the release of inflammatory factors by blocking the PD-1/PD-L1 signal pathway. (A) The concentration of IL-6 and TNF-α was determined by enzyme-linked immunosorbent assay. (B) The expression level of SHP-2, PI3K, p-AKT and AKT was detected by western blotting. *P<0.05 vs. control; **P<0.01 vs. control. (C) The expression of PD-1 in CD8^{+} T cells and the expression of PD-L1 in DC cells were determined by reverse transcription-quantitative PCR assay. **P<0.01 vs. pc-DNA3.1-NC. (D) The expression levels of SHP-2, PI3K, p-AKT and AKT in the co-cultural system of DC cells (wild type or PD-L1 overexpressed) and CD8^{+} T cells (wild type or PD-1 overexpressed) in the presence of TFL was determined by western blotting. **P<0.01 vs. control; $^{\#\#}$P<0.01 vs. TFL. IL-6, interleukin-6; TNF-α, tumor necrosis factor-α; p-, phosphorylated-; DC, dendritic cells; NK cells; natural killer cells; NC, negative control; PD-1, programmed death 1; PD-L1, programmed cell death ligand 1; TFL, Tong-fu-li-fei.

cells, as well as the assuasive inflammation caused by CLP. These *in-vivo* data claimed a potential therapeutic effect of TFL on intestinal injury induced by sepsis. However, more detailed investigation will be explored in future work to confirm the pharmacological function, including the evaluation of immunosuppression-associated cells, clinical chemistry of peripheral blood and the determination of an optimized dosage.

Pro-inflammatory reaction and anti-inflammatory reaction are reported to be simultaneously involved in the pathological procedure of sepsis (29). Currently, systemic inflammation caused by sepsis can be treated as the development of medicine. However, in the advanced stage of sepsis, patients will be experienced with the immunosuppression state, which is characterized by low immune reaction or no response. The secondary infection and associated complications will be induced as the sensitivity and clearance of immune system to the pathogenic bacteria decreases (30,31). Roquilly *et al* (32) reported that the antigen-presentation ability of both macrophages and DCs was suppressed in rats with sepsis, accompanied with increased production of Treg cells and transforming factor-β, indicating a significant immunosuppression state induced by sepsis. PD-1/PD-L1 is a classic signaling pathway that mediates the immunosuppression system. The activation of effective T cells can be suppressed by binding with PD-L1 using PD-1 expression on T cells to maintain the balance of immune system. It is reported that the survival rate of rats with sepsis could be elevated as the release of interferon (IFN)-γ and the apoptotic level are inhibited, which were achieved by blocking the PD-1/PD-L1 signaling pathway (33). The effects of blocking the PD-1/PD-L1 signaling pathway have also been verified by clinical administrating anti-PD-1 or anti-PD-L1 antibodies to the patients with sepsis, with decreased apoptosis and increased production of IFN-γ and IL-2 (34). SHP-2 and PI3K/AKT are main downstream signal pathways of PD-1/PD-L1 that exert the immunosuppression effects (35,36). In the present study, accompanied with inflammation detection, it was found that the SHP-2 and PI3K/AKT signal pathway were significantly activated by CLP, indicating a significant immunosuppression induced by activated PD-1/PD-L1 signal pathway. By the introduction of TFL, especially at high and moderate dosage, the activated SHP-2 and PI3K/AKT signaling pathway were significantly suppressed, indicating an inhibitory effect on the PD-1/PD-L1 signaling pathway and an effect on the activation of immune system. Further mechanistic study showed that SHP-2 and PI3K/AKT signal pathway in the co-cultural system of DC cells and $CD8^+$ T cells was significantly inhibited by the introduction of TFL. Interestingly, the production of IL-6 and TNF-α in the co-cultural system was found to be elevated by the treatment of TFL, which was not consistent with the *in-vivo* data. It was suspected that the inflammatory situation *in-vivo* is more complicated compared with that *in-vitro* and the balance of the immunity in the CLP-induced rats might be maintained by TFL, so that the decreased production of inflammatory factors was accompanied by improved sepsis symptoms. In the *in-vitro* study, the release of the inflammatory factors might only be regulated by the PD-1/PD-L1 signaling pathway, which was inhibited by TFL and resulting in an immunopotentiation in CD 8^+ T cells. The hypothesis was further verified by activating the PD-1/PD-L1 signal pathway in the presence of TFL. However, further investigations will be performed on the direct interaction between TFL and the PD-1/PD-L1 signaling pathway to further verify our hypothesis. In addition, these data indicated that the PD-1/PD-L1 interaction between DC and $CD8^+$ T cells was blocked by TFL. However, the evidence with these preliminary data from the present study is not sufficient to directly claim that the anti-sepsis effect of TFL resulted from blocking the PD-1/PD-L1 signaling pathway. Further investigations at the molecular level will be explored to better understand the association between the therapeutic effects of TFL against sepsis and the immunosuppression induced by blocking the PD-1/PD-L1 signaling pathway.

Taken together, the data from the present study indicate that Tong-fu-li-fei decoction may attenuate immunosuppression to protect the intestinal mucosal barrier in sepsis via inhibiting the PD-1/PD-L1 signaling pathway.

Acknowledgements

Not applicable.

Funding

This work was supported by grants from the National Natural Science Foundation of China (grant no. 81860846) and Science and Technology Project of Guiyang City [grant no. (2019)9-2-12].

Availability of data and materials

The datasets used and/or analyzed during the current study are available from the corresponding author on reasonable request.

Authors' contributions

BL conceived and designed the present study. LL, SZ and QL performed the experiments and analyzed the data. LC interpreted the data and wrote the manuscript. BL and LC confirm the authenticity of all the raw data. All authors read and approved the final manuscript, and agree to be accountable for all aspects of the research in ensuring that the accuracy or integrity of any part of the work are appropriately investigated and resolved.

Ethics approval and consent to participate

All animal experiments involved in this manuscript were authorized by the ethical committee of First Affiliated Hospital of Guizhou University of Chinese Medicine (approval date, 10 December 2019; approval no. GUCM-FAH-20191210) and was carried out according to the guidelines for care and use of laboratory animals, as well as to the principles of laboratory animal care and protection.

Patient consent for publication

Not applicable.

Competing interests

The authors declare that they have no competing interests.

References

1. Uchimido R, Schmidt EP and Shapiro NI: The glycocalyx: A novel diagnostic and therapeutic target in sepsis. Crit Care 23: 16, 2019.
2. Riedemann NC, Guo RF and Ward PA: The enigma of sepsis. J Clin Invest 112: 460-467, 2003.
3. Osuchowski MF, Welch K, Siddiqui J and Remick DG: Circulating cytokine/inhibitor profiles reshape the understanding of the SIRS/CARS continuum in sepsis and predict mortality. J Immunol 177: 1967-1974, 2006.
4. Gotts JE and Matthay MA: Sepsis: Pathophysiology and clinical management. BMJ 353: i1585, 2016.
5. Hotchkiss RS, Tinsley KW, Swanson PE, Schmieg RE Jr, Hui JJ, Chang KC, Osborne DF, Freeman BD, Cobb JP, Buchman TG and Karl IE: Sepsis-induced apoptosis causes progressive profound depletion of B and $CD4^+$ T lymphocytes in humans. J Immunol 166: 6952-6963, 2001.
6. Munoz C, Carlet J, Fitting C, Misset B, Bleriot JP and Cavaillon JM: Dysregulation of in vitro cytokine production by monocytes during sepsis. J Clin Invest 88: 1747-1754, 1991.
7. Wang HW, Yang W, Gao L, Kang JR, Qin JJ, Liu YP and Lu JY: Adoptive transfer of bone marrow-derived dendritic cells decreases inhibitory and regulatory T-cell differentiation and improves survival in murine polymicrobial sepsis. Immunology 145: 50-59, 2015.
8. Bouras M, Asehnoune K and Roquilly A: Contribution of dendritic cell responses to sepsis-induced immunosuppression and to susceptibility to secondary pneumonia. Front Immunol 9: 2590, 2018.
9. Manjuck J, Saha DC, Astiz M, Eales LJ and Rackow EC: Decreased response to recall antigens is associated with depressed costimulatory receptor expression in septic critically ill patients. J Lab Clin Med 135: 153-160, 2000.
10. Le Tulzo Y, Pangault C, Amiot L, Guilloux V, Tribut O, Arvieux C, Camus C, Fauchet R, Thomas R and Drénou B: Monocyte human leukocyte antigen-DR transcriptional down-regulation by cortisol during septic shock. Am J Respir Crit Care Med 169: 1144-1151, 2004.
11. Ishida Y, Agata Y, Shibahara K and Honjo T: Induced expression of PD-1, a novel member of the immunoglobulin gene superfamily, upon programmed cell death. EMBO J 11: 3887-3895, 1992.
12. Keir ME, Butte MJ, Freeman GJ and Sharpe AH: PD-1 and its ligands in tolerance and immunity. Annu Rev Immunol 26: 677-704, 2008.
13. Naidoo J, Schindler K, Querfeld C, Busam K, Cunningham J, Page DB, Postow MA, Weinstein A, Lucas AS, Ciccolini KT, *et al*: Autoimmune bullous skin disorders with immune checkpoint inhibitors targeting PD-1 and PD-L1. Cancer Immunol Res 4: 383-389, 2016.
14. Dai S, Jia R, Zhang X, Fang Q and Huang L: The PD-1/PD-Ls pathway and autoimmune diseases. Cell Immunol 290: 72-79, 2014.
15. Brunner-Weinzierl MC and Rudd CE: CTLA-4 and PD-1 control of T-Cell motility and migration: Implications for tumor immunotherapy. Front Immunol 9: 2737, 2018.
16. Chen L, Li L, Han Y, Lv B, Zou S and Yu Q: Tong-fu-li-fei decoction exerts a protective effect on intestinal barrier of sepsis in rats through upregulating ZO-1/occludin/claudin-1 expression. J Pharmacol Sci 143: 89-96, 2020.
17. Fu J, Li G, Wu X and Zang B: Sodium butyrate ameliorates intestinal injury and improves survival in a rat model of cecal ligation and puncture-induced sepsis. Inflammation 42: 1276-1286, 2019.
18. Rendon JL, Li X, Akhtar S and Choudhry MA: Interleukin-22 modulates gut epithelial and immune barrier functions following acute alcohol exposure and burn injury. Shock 39: 11-18, 2013.
19. Ke J, Bian X, Liu H, Li B and Huo R: Edaravone reduces oxidative stress and intestinal cell apoptosis after burn through up-regulating miR-320 expression. Mol Med 25: 54, 2019.
20. Livak KJ and Schmittgen TD: Analysis of relative gene expression data using real-time quantitative PCR and the 2(-Delta Delta C(T)) method. Methods 25: 402-408, 2001.
21. Wichterman KA, Baue AE and Chaudry IH: Sepsis and septic shock-a review of laboratory models and a proposal. J Surg Res 29: 189-201, 1980.
22. Singer M, Deutschman CS, Seymour CW, Shankar-Hari M, Annane D, Bauer M, Bellomo R, Bernard GR, Chiche JD, Coopersmith CM, *et al*: The Third International consensus definitions for sepsis and septic shock (Sepsis-3). JAMA 315: 801-810, 2016.
23. Shankar-Hari M, Harrison DA, Rubenfeld GD and Rowan K: Epidemiology of sepsis and septic shock in critical care units: Comparison between sepsis-2 and sepsis-3 populations using a National critical care database. Br J Anaesth 119: 626-636, 2017.
24. Thomas H: Sepsis: Bile acids promote inflammation in cholestasis-associated sepsis. Nat Rev Gastroenterol Hepatol 14: 324-325, 2017.
25. Rosenthal MD and Moore FA: Persistent inflammation, immunosuppression, and catabolism: Evolution of multiple organ dysfunction. Surg Infect (Larchmt) 17: 167-172, 2016.
26. Zhu Y, Wang Y, Teng W, Shan Y, Yi S, Zhu S and Li Y: Role of aquaporin-3 in intestinal injury induced by sepsis. Biol Pharm Bull 42: 1641-1650, 2019.
27. Chang X, Wang LL, Lian SJ, Tang Q, Chen P and Wang H: Effect of oral glutamine on intestinal barrier function in young rats with endotoxemia. Zhongguo Dang Dai Er Ke Za Zhi 12: 809-811, 2010 (In Chinese).
28. Meena AS, Shukla PK, Sheth P and Rao R: EGF receptor plays a role in the mechanism of glutamine-mediated prevention of alcohol-induced gut barrier dysfunction and liver injury. J Nutr Biochem 64: 128-143, 2019.
29. Chao CY, Sung PJ, Wang WH and Kuo YH: Anti-inflammatory effect of Momordica charantia in sepsis mice. Molecules 19: 12777-12788, 2014.
30. Venet F, Rimmele T and Monneret G: Management of sepsis-induced immunosuppression. Crit Care Clin 34: 97-106, 2018.
31. Venet F and Monneret G: Advances in the understanding and treatment of sepsis-induced immunosuppression. Nat Rev Nephrol 14: 121-137, 2018.
32. Roquilly A, McWilliam HEG, Jacqueline C, Tian Z, Cinotti R, Rimbert M, Wakim L, Caminschi I, Lahoud MH, Belz GT, *et al*: Local modulation of antigen-presenting cell development after resolution of pneumonia induces long-term susceptibility to secondary infections. Immunity 47: 135-147 e5, 2017.
33. Chang KC, Burnham CA, Compton SM, Rasche DP, Mazuski RJ, McDonough JS, Unsinger J, Korman AJ, Green JM and Hotchkiss RS: Blockade of the negative co-stimulatory molecules PD-1 and CTLA-4 improves survival in primary and secondary fungal sepsis. Crit Care 17: R85, 2013.
34. Chang K, Svabek C, Vazquez-Guillamet C, Sato B, Rasche D, Wilson S, Robbins P, Ulbrandt N, Suzich J, Green J, *et al*: Targeting the programmed cell death 1: Programmed cell death ligand 1 pathway reverses T cell exhaustion in patients with sepsis. Crit Care 18: R3, 2014.
35. Li J, Jie HB, Lei Y, Gildener-Leapman N, Trivedi S, Green T, Kane LP and Ferris RL: PD-1/SHP-2 inhibits Tc1/Th1 phenotypic responses and the activation of T cells in the tumor microenvironment. Cancer Res 75: 508-518, 2015.
36. Zhao R, Song Y, Wang Y, Huang Y, Li Z, Cui Y, Yi M, Xia L, Zhuang W, Wu X and Zhou Y: PD-1/PD-L1 blockade rescue exhausted $CD8^+$ T cells in gastrointestinal stromal tumours via the PI3K/Akt/mTOR signalling pathway. Cell Prolif 52: e12571, 2019.